

21 **Abstract**

22 Antimicrobial combinations have been proven to be a promising approach in the
23 confrontation with multi-drug resistant bacterial pathogens, owing to enhancement of
24 antibacterial efficacy, deceleration of resistance development rate and mitigation of side
25 effects by lowering the doses of two drugs. In the present study, we report that combination
26 of furazolidone (FZ) and other nitrofurans with a secondary bile salt, Sodium Deoxycholate
27 (DOC), generates a profound synergistic effect on growth inhibition and lethality in
28 enterobacteria, including *Escherichia coli*, *Salmonella*, *Citrobacter gillenii* and *Klebsiella*
29 *pneumoniae*. Taking *E. coli* as the model organism to study the mechanism of DOC-FZ
30 synergy, we found that the synergistic effect involves FZ-mediated inhibition of efflux pumps
31 that normally remove DOC from bacterial cells. We further show that the FZ-mediated nitric
32 oxide production contributes to the synergistic effect. This is to our knowledge the first report
33 of nitrofurans-DOC synergy against Gram-negative bacteria.

34 **Introduction**

35 Antimicrobial resistance (AMR) is one of the most serious threats with which humans have
36 been confronted. A UK-Prime-Minister-commissioned report in 2014 estimated that AMR,
37 without appropriate interventions, will cause globally 10 million deaths per annum with a
38 cumulative loss of US \$100 trillion by 2050 (1). In this dire context, alternative approaches
39 are urgently needed besides traditional discovery of novel antibiotics, in which antimicrobial
40 combinations have been proven to be a promising approach with some widely accepted
41 advantages, including enhancement of antimicrobial efficacy, deceleration of the rate of
42 resistance and alleviation of side effects (2, 3). Moreover, this approach could amplify the
43 significance of ongoing antimicrobial discovery programs; particularly the advent of any
44 novel antimicrobial compound would bring about a large number of possible double

45 combinations with existing antimicrobial agents to be evaluated, let alone triple and
46 quadruple combinations.

47 Sodium Deoxycholate (DOC) (Figure 1E) is a facial amphipathic compound in bile, which is
48 secreted into the duodenum to aid lipid digestion and confer some antimicrobial protection
49 (4). Though extensive research has been conducted to elucidate the interaction between
50 DOC, either alone or in bile mixture, and enteric bacteria, the mode of its antimicrobial action
51 remains elusive. It was suggested that DOC could attack multiple cellular targets, including
52 disturbing cell membranes, causing DNA damage, triggering oxidative stress and inducing
53 protein misfolding (4-6). Nonetheless, Gram-negative bacteria such as *Escherichia coli* and
54 *Salmonella* are highly resistant to DOC by many mechanisms such as employment of diverse
55 active efflux pumps, down-regulation of outer membrane porins and activation of various
56 stress responses (5, 7-10).

57 The 5-nitrofurans are an old class of synthetic antimicrobials, clinically introduced in the
58 1940s and 1950s (11); several are commercially available, including furazolidone (FZ),
59 nitrofurantoin (NIT) and nitrofurazone (NFZ) (Figure 1). FZ is used to treat bacterial
60 diarrhea, giardiasis and as a component in combinatorial therapy for *Helicobacter pylori*
61 infections; NIT and NFZ are used for urinary tract infections and topical applications,
62 respectively (12). They are prodrugs which require reductive activation mediated largely by
63 two type-I oxygen-insensitive nitroreductases, NfsA and NfsB. These two enzymes perform
64 stepwise 2-electron reduction of the nitro moiety of the compound into the nitroso and
65 hydroxylamino intermediates and biologically inactive amino-substituted product (13, 14).
66 The detailed mechanism of how bacterial cells are killed by the reactive intermediate has yet
67 to be clarified. Nevertheless, it has been proposed that the hydroxylamino derivatives could
68 trigger DNA lesions, disrupt protein structure and arrest RNA and protein biosynthesis (15-
69 19). Some reports also suggested that nitric oxide could be generated during the activation

70 process, thus inhibiting electron transport chain of bacterial cells though clear evidence for
71 that is not available as yet (20, 21).

72 In this study, we have characterized interaction of DOC with FZ and three other related
73 nitrofurans against a range of enterobacteria. We identified the underlying mechanism of
74 DOC-FZ synergy using *E. coli* K12 as a model organism.

75 **Results**

76 **The synergy between DOC and 5-nitrofurans against enterobacteria**

77 To evaluate the synergy between DOC and FZ, the checkerboard growth inhibition assays
78 were performed for a range of enterobacteria, including *Salmonella enterica* sv.
79 Typhimurium LT2, *Citrobacter gillenii*, *Klebsiella pneumoniae* and two *E. coli* antibiotic-
80 resistant strains (streptomycin-resistant and streptomycin/ampicillin-resistant). DOC and FZ
81 act synergistically in inhibiting the growth of the microorganisms listed (Figure 2), with FICI
82 ranging from 0.125 in streptomycin-resistant *E. coli* strain (Figure 2A) to 0.35 in *K.*
83 *pneumoniae* (Figure 2F). DOC-FZ synergy was also observed against two *E. coli* pathogenic
84 strains (*E. coli* strain O157 and urinary tract infection strain P50; Figure S1). It is worth
85 noting that, when used alone, very high DOC concentrations were required to exert an
86 equivalent effect on inhibiting the growth of these Gram-negative enterobacteria, reflecting
87 the inherent resistance to DOC in these bacteria thanks to their impermeable outer membrane
88 and active efflux pumps, which prevent the intracellular accumulation of toxic xenobiotics.

89 We also examined the interaction between DOC and other nitrofurans compounds, including
90 NIT, NFZ and CM4 (a 5-nitrofurans compound we found during an antimicrobial synergy
91 screening campaign against *E. coli*, Figure 1D) in all the bacterial species mentioned above.
92 We found that NIT, NFZ and CM4 were synergistic with DOC in *E. coli* laboratory strain

93 (Figure 4), *Citrobacter gillenii* (Figure S2) and *Salmonella* Typhimurium LT2 (Figure S3)
94 but indifferent in *K. pneumoniae* isolate (Figure S4).

95 To elaborate the interaction between DOC and FZ in terms of bactericidal effects, the time-
96 kill assay was employed. Streptomycin-resistant *E. coli* K12 laboratory strain K1508 and *S.*
97 *enterica* serovar Typhimurium strain LT2 were exposed to sub-inhibitory concentrations of
98 DOC (2500 µg/mL) alone, or FZ (0.5 × MIC) alone, or combination of the two drugs at such
99 sub-inhibitory concentrations, over a 24 h period. The sample was taken at different time
100 points and the surviving bacteria were titrated on the antimicrobial-free plates. Centrifugation
101 and resuspension were applied for each sample to eliminate the antimicrobial carryover
102 before plating. After 24 h, the total cell count in the sample treated with the DOC-FZ
103 combination was about six to seven orders of magnitude lower than that in the sample treated
104 with either DOC or FZ alone for both *E. coli* and *Salmonella* (Figure 3), demonstrating the
105 synergy in bacterial killing between DOC and FZ.

106 **The role of AcrAB-TolC efflux pump in synergistic interaction between DOC and** 107 **nitrofurans**

108 One commonly accepted principle is that the synergy between two drugs is a consequence of
109 one drug suppressing bacterial physiological pathways that mediate resistance to the other
110 one. It has been reported that DOC could be expelled out of the cell via a wide range of efflux
111 pumps, in which the tripartite efflux system AcrAB-TolC plays the major role (7, 9) . This
112 led us to hypothesize that FZ inhibits the activity of efflux pumps, thus allowing intracellular
113 accumulation of DOC to exert its lethal effect. If this scenario were true, disruption of the
114 function of efflux pumps by mutation was expected to make this activity of FZ redundant,
115 thus reducing the interaction index (FICI) in the mutant strains.

116 To validate this model in *E. coli*, the checkerboard assay was performed on the strains
117 containing deletions of individual genes encoding the AcrAB-TolC efflux pump system,
118 $\Delta tolC$ and $\Delta acrA$. Deletion of *tolC* caused a shift from the synergistic interaction between
119 DOC and FZ in the wild type (FICI = 0.125) to indifferent interaction (FICI=0.75; Figure
120 4A). The $\Delta acrA$ mutant exhibited a 3-fold decrease in the FICI index relative to the isogenic
121 wild type strain. Such changes were also observed for the interaction between DOC and other
122 nitrofurans, NIT, NFZ or CM4 (Figure 4BCD).

123 To confirm that these observations were conferred by direct effect of the *tolC* and *acrA*
124 deletion, rather than indirect effects of other genes or proteins, complementation of the
125 corresponding deletion mutations by plasmid-expressed *tolC* and *acrA* was performed. To
126 compensate for the multiple copies of plasmid-containing genes, complementation was
127 carried out at a low level of expression, nevertheless it completely restored the strong synergy
128 between DOC and FZ in these complemented strains (Figure 5). These findings collectively
129 support the model that the efflux pumps act as the interacting point for the synergy between
130 DOC and FZ.

131 An intriguing question to be unraveled is how FZ could negatively influence the action of
132 efflux pumps. We hypothesized that FZ could lower the energy supply to efflux pumps by
133 mediating an increase in concentration of nitric oxide (NO). To verify the proposed model,
134 the interaction between DOC and FZ in the *E. coli* strain with increased expression of protein
135 Hmp (the *E. coli* nitric oxide dioxygenase) was inspected. The rationale for this is that
136 overexpression of Hmp protein would increase detoxification of NO by conversion into
137 benign NO_3^- ions, thus relieving the effect exerted by NO (22) . If NO was involved in the
138 mechanism of the interaction between the two drugs, the synergy degree between them was
139 expected to decrease with an increased abundance of Hmp proteins. In agreement with this

140 hypothesis, overexpression of *hmp* was found to suppress the synergy between DOC and FZ
141 by a factor of 3 (Figure 6). This finding supports the model that NO generated during FZ
142 metabolism participates in the inhibition of electron transport chain (23), with the secondary
143 effect of inhibiting the function of efflux pumps which are dependent on the electron
144 transport chain for their activity.

145 **Discussion**

146 The widespread emergence of antimicrobial drug resistance and the drying pipeline of
147 antibiotics for Gram-negative pathogens imposed an urgency to seek for novel approaches to
148 combat these pathogens. Capitalization on drug combinations is one of the promising
149 approaches to design novel therapies that will allow application of antimicrobials which have
150 heretofore been ineffective against Gram-negative bacteria at concentrations that are
151 acceptable for medical treatments. In the present study, we describe the synergistic
152 interaction between DOC and FZ in a range of enterobacteria in terms of growth inhibition
153 and/or lethality. These findings offer two major implications. Firstly, Gram-negative bacteria,
154 such as *E. coli* and *Salmonella* have evolved to be highly resistant to bile salts, including
155 DOC (10); inclusion of an active agent, such as FZ or other 5-nitrofurans could revitalize
156 DOC in the battle against such formidable pathogens. This discovery raises a possibility of
157 using synergistic combinations in enabling use of antimicrobials that are on their own
158 ineffective against Gram-negative bacteria at sub-toxic concentrations, for treatment of
159 infections caused by these resilient organisms.

160 Secondly, DOC and other bile salts are inherently present at varying concentrations along the
161 gastrointestinal tract. The efficacy of any drug dedicated to treat intestinal infections would
162 depend on physicochemical properties of the local environment in which interaction with bile
163 salts is one important factor. The synergy between DOC and FZ described here partly

164 explains the success of using FZ in curing bacterial diarrhea (12, 24). To further highlight
165 such an interaction, it has also been reported that rifaximin, an RNA synthesis inhibitor,
166 worked more efficiently in treating diarrhea-producing *E. coli* in the intestine than in the
167 colon, due to the difference in the bile salt concentration (25). From these observations, we
168 propose the co-administration of DOC and FZ to treat bacterial diarrhea for the patients who
169 have low intestinal concentrations of DOC due to malnourishment, disorders in enterohepatic
170 circulation or intestinal absorption (4). Nonetheless, further investigations are required to
171 justify the validity of that proposal.

172 In this study, we have also provided some insights into the underlying mechanism of the
173 synergy between DOC and FZ in their antibacterial action against *E. coli* as a model Gram-
174 negative bacterium. We showed that disruption of *tolC* or *acrA* gene caused a considerable
175 decrease in the synergy between DOC and FZ in the corresponding mutants. The TolC
176 protein, whose removal disrupts the synergy more strikingly, appears to be the key
177 determinant of synergy.

178 The observed difference in the susceptibility to DOC/FZ combination between $\Delta tolC$ and
179 $\Delta acrA$ mutants is in agreement with the fact that the TolC protein is shared by at least seven
180 multidrug efflux pumps, while AcrA protein acts as the periplasmic connecting bridge for
181 only two (26). Thus, deletion of *tolC* gene is expected to give rise to a more pronounced
182 effect on the loss of efflux activities than deletion of *acrA* gene.

183 Of great interest is how FZ could influence the activity of efflux pumps. The obtained
184 findings indicate that more than two efflux pumps (AcrAB-TolC and AcrAD-TolC systems)
185 were affected by FZ. This observation is reminiscent of a common mechanism which could
186 affect a wide range of efflux pumps simultaneously, namely proton motive force. It has been
187 suggested that nitrofurantoin compounds during reductive activation might generate nitric oxide

188 (NO) which subsequently inhibits the electron transport chain (ETC), diminishing the proton
189 motive force across the cytoplasmic membrane (20, 21, 23, 27). As a result, many efflux
190 pumps would be de-energized, and become less efficient in extruding toxic compounds.
191 However, NO generation from nitrofurans in bacterial cells remains to be speculative since
192 the trace of NO has yet to be detected using either biochemical or NO-sensing fluorescence
193 methods, possibly due to the detection limit of the used methods or rapid conversion of NO
194 into other compounds (20, 21). In the present work, we provide evidence for the contribution
195 of NO in the interaction between DOC and FZ via the observation that overexpression of
196 NO-detoxifying enzyme Hmp decreased the synergistic interaction between the two agents.
197 Since some DOC-FZ synergy was still retained after NO-detoxification, other mechanisms,
198 including direct inhibition of the ETC by activated FZ, are involved in the efflux pump
199 inhibition.

200 In conclusion, we report the synergy between FZ and DOC in inhibiting and/or killing
201 different enterobacterial species. In the terms of underlying mechanisms, much evidence
202 supports the model that FZ negatively influences the activity of many efflux pumps such that
203 DOC could accumulate inside the cell to exert its cytotoxic effect. One possible route is via
204 FZ-derived NO which inhibits the electron transport chain, thus dissipating the energy supply
205 for efflux machineries. Nonetheless, other mechanisms might be involved, remaining to be
206 elucidated.

207 **Materials and methods**

208 **Bacterial strains, growth conditions and antibiotics**

209 All bacterial strains and plasmids used in this study were described in **Table 1** and **Table 2**.
210 The introduction of the *kan^R* gene deletion mutations into the wild type strain K1508 from the
211 corresponding Keio collection *E. coli* K12 knock-out strains (28) was performed using phage

212 P1 transduction, according to the standard procedures (29). To eliminate potential polar
213 effects on downstream genes in the operon, the FRT-flanked *kan^R* cassette was then removed
214 using FLP-mediated recombination as previously described (30). Plasmids derived from the
215 pCA24N bearing the gene of interest were purified from *E. coli* strains of the ASKA
216 collection containing ORF expression constructs derived from this organism (31) using the
217 ChargeSwitch-Pro Plasmid Miniprep Kit (Thermo Fisher Scientific). The plasmid DNA was
218 then chemically transformed into specific *E. coli* strains for further work (32). Expression
219 from the pCA24N vector is driven from a T5-*lac* chimeric promoter. In the case of membrane
220 protein expression (TolC and AcrA) the basal expression from uninduced promoter was used
221 in complementation experiments to avoid toxicity of membrane protein overexpression due to
222 the Sec system saturation, whereas expression of Hmp (a cytosolic NO-detoxifying protein)
223 was induced by 1 mM IPTG.

224 Bacterial culture was grown in 2xYT medium (BD Difco) at 37°C with shaking at 200 rpm.
225 For preparation of exponential phase cells, fresh overnight culture was 100-fold diluted and
226 incubated to reach the OD_{600nm} of about 0.1-0.3. This cell suspension was then diluted to the
227 desirable concentration depending on specific purposes. Sodium Deoxycholate was a kind
228 gift from New Zealand Pharmaceuticals Ltd. Antibiotics used in this study were purchased
229 from GoldBio. CM4 was purchased from Enamine (catalog number Z49681516).

230 **Checkerboard assay**

231 The checkerboard assay for DOC and FZ was performed on the Corning 384-well microtiter
232 plate with the concentration of DOC ranging from 20000 µg/mL to 0 µg/mL and the
233 concentration of FZ ranging from 10 µg/mL to 0 µg/mL, prepared by 2-fold serial dilution.
234 The concentration range could be adjusted depending on the sensitivity of different bacterial
235 strains and the types of nitrofurans to cover at least 2 × MIC to 0.06 × MIC of each drug.

236 Each well contained the starting inoculum of approximately 10^6 CFU/mL, 2 % DMSO and
237 the predefined concentration of each drug in the total volume of 50 μ L. The wells containing
238 no drugs and 10 μ g/mL tetracycline were used as negative controls and positive controls,
239 respectively. After dispensing the reagents, the plate was pulse centrifuged at $1000 \times g$ to
240 eliminate any bubbles. The plate was then incubated at 30°C and the $\text{OD}_{600\text{nm}}$ of the sample
241 was monitored for every 1 h within 24h using MultiskanTM GO Microplate
242 Spectrophotometer (Thermo Scientific). Each combination was performed in triplicate. The
243 growth inhibition with the cut-off value of 90 % at the time point 24 h was used to define the
244 MIC of the drug used alone or in combination (33). The fractional inhibitory concentration
245 index (FICI) for the two drugs was calculated as follows:

$$\text{FICI} = \frac{\text{MIC}_{\text{DOCcom}}}{\text{MIC}_{\text{DOCalone}}} + \frac{\text{MIC}_{\text{FZcom}}}{\text{MIC}_{\text{FZalone}}}$$

$\text{MIC}_{\text{DOCcom}}$ and $\text{MIC}_{\text{FZcom}}$: MIC of DOC and FZ when tested in combination

$\text{MIC}_{\text{DOCalone}}$ and $\text{MIC}_{\text{FZalone}}$: MIC of DOC and FZ when tested individually

246 The interaction between two drugs was interpreted as synergistic if FICI was ≤ 0.5 ,
247 indifferent if it was > 0.5 and ≤ 4 , and antagonistic if it was > 4 (34).

248 **Time kill assay**

249 Exponential phase bacterial culture at about 10^6 CFU/ml was prepared in the final volume of
250 10 mL containing 2 % DMSO plus DOC at 2500 μ g/ml alone or FZ at $0.5 \times \text{MIC}$ μ g/mL
251 alone or both drugs. The treatments containing no drug were used as negative controls. The
252 samples were incubated at 30°C with shaking at 200 rpm. At the time points of 0 h, 2 h, 4 h, 6
253 h, 8 h and 24 h, 500 μ L were taken from each treatment and centrifuged at $10000 \times g$ for 15
254 min before being re-suspended in 100 μ L maximum recovery diluent (0.1 % peptone, 0.85 %

255 NaCl). 10 μ L of serial dilutions was plated on 2xYT agar followed by overnight incubation at
256 37°C to determine the cell count. Each treatment was performed in triplicate. The
257 antimicrobial interaction was interpreted as synergistic if the combinatorial treatment caused
258 a killing efficiency ≥ 2 log higher than the most active agent (35).

259 **Acknowledgements**

260 We thank Dr. Anne Midwinter, School of Veterinary Sciences, Massey University, for
261 providing a *E. coli* human O157 isolate and New Zealand Veterinary Pathology Ltd. for an
262 isolate of a canine *E. coli* UPEC strain (P50). We are grateful to Fraser Glickman from
263 Rockefeller University High Throughput and Spectroscopy Resource Center for hosting and
264 advice on small-molecule drug screen of a synergy screen and to the National BioResource
265 Project (NBRP) via Genetics Strains Research Center, National Institute of Genetics, Japan,
266 for providing the ASKA collection. The Keio Collection was purchased from Dharmacon *via*
267 ThermoFisher (Australia).

268 **Funding information**

269 Vuong Van Hung Le has received funding from Callaghan Innovation PhD Scholarship. This
270 work was supported by Massey University, the New Zealand Ministry of Business,
271 Innovation and Employment and New Zealand Pharmaceuticals LTD.

272 **References**

- 273 1. **O'Neill J, Review-team.** 2014. Antimicrobial resistance: tackling a crisis for the
274 health and wealth of nations. <https://amr-review.org/>,
- 275 2. **Bollenbach T.** 2015. Antimicrobial interactions: mechanisms and implications for
276 drug discovery and resistance evolution. *Curr Opin Microbiol* **27**:1-9.

- 277 3. **Taneja N, Kaur H.** 2016. Insights into newer antimicrobial agents against Gram-
278 negative bacteria. *Microbiol Insights* **9**:9-19.
- 279 4. **Begley M, Gahan CG, Hill C.** 2005. The interaction between bacteria and bile.
280 *FEMS Microbiol Rev* **29**:625-651.
- 281 5. **Merritt ME, Donaldson JR.** 2009. Effect of bile salts on the DNA and membrane
282 integrity of enteric bacteria. *J Med Microbiol* **58**:1533-1541.
- 283 6. **Cremers CM, Knoefler D, Vitvitsky V, Banerjee R, Jakob U.** 2014. Bile salts act
284 as effective protein-unfolding agents and instigators of disulfide stress in vivo. *Proc*
285 *Natl Acad Sci USA* **111**:E1610-E1619.
- 286 7. **Nishino K, Yamaguchi A.** 2001. Analysis of a complete library of putative drug
287 transporter genes in *Escherichia coli*. *J Bacteriol* **183**:5803-5812.
- 288 8. **Van Bambeke F, Glupczynski Y, Plesiat P, Pechere JC, Tulkens PM.** 2003.
289 Antibiotic efflux pumps in prokaryotic cells: occurrence, impact on resistance and
290 strategies for the future of antimicrobial therapy. *J Antimicrob Chemother* **51**:1055-
291 1065.
- 292 9. **Paul S, Alegre KO, Holdsworth SR, Rice M, Brown JA, McVeigh P, Kelly SM,**
293 **Law CJ.** 2014. A single-component multidrug transporter of the major facilitator
294 superfamily is part of a network that protects *Escherichia coli* from bile salt stress.
295 *Mol Microbiol* **92**:872-884.
- 296 10. **Sistrunk JR, Nickerson KP, Chanin RB, Rasko DA, Faherty CS.** 2016. Survival
297 of the fittest: how bacterial pathogens utilize bile to enhance infection. *Clin Microbiol*
298 *Rev* **29**:819-836.
- 299 11. **Chamberlain RE.** 1976. Chemotherapeutic properties of prominent nitrofurans. *J*
300 *Antimicrob Chemother* **2**:325-336.

- 301 12. **Vass M, Hruska K, Franek M.** 2008. Nitrofurantoin antibiotics: a review on the
302 application, prohibition and residual analysis. *Vet Med-Czech* **53**:469-500.
- 303 13. **Whiteway J, Koziarz P, Veall J, Sandhu N, Kumar P, Hoecher B, Lambert IB.**
304 1998. Oxygen-insensitive nitroreductases: analysis of the roles of *nfsA* and *nfsB* in
305 development of resistance to 5-nitrofurantoin derivatives in *Escherichia coli*. *J Bacteriol*
306 **180**:5529-5539.
- 307 14. **Sandegren L, Lindqvist A, Kahlmeter G, Andersson DI.** 2008. Nitrofurantoin
308 resistance mechanism and fitness cost in *Escherichia coli*. *J Antimicrob Chemother*
309 **62**:495-503.
- 310 15. **McCalla DR.** 1979. Nitrofurans, p 176-213. *In* Hahn FE (ed), Mechanism of Action
311 of Antibacterial Agents doi:10.1007/978-3-642-46403-4. Springer Berlin Heidelberg,
312 Heidelberg, Germany.
- 313 16. **McOsker CC, Fitzpatrick PM.** 1994. Nitrofurantoin: mechanism of action and
314 implications for resistance development in common uropathogens. *J Antimicrob*
315 *Chemother* **33 Suppl A**:23-30.
- 316 17. **Bertenyi KK, Lambert IB.** 1996. The mutational specificity of furazolidone in the
317 *lacI* gene of *Escherichia coli*. *Mutat Res* **357**:199-208.
- 318 18. **Roldan MD, Perez-Reinado E, Castillo F, Moreno-Vivian C.** 2008. Reduction of
319 polynitroaromatic compounds: the bacterial nitroreductases. *FEMS Microbiol Rev*
320 **32**:474-500.
- 321 19. **Ona KR, Courcelle CT, Courcelle J.** 2009. Nucleotide excision repair is a
322 predominant mechanism for processing nitrofurantoin-induced DNA damage in
323 *Escherichia coli*. *J Bacteriol* **191**:4959-4965.
- 324 20. **Kumar M, Adhikari S, Hurdle JG.** 2014. Action of nitroheterocyclic drugs against
325 *Clostridium difficile*. *Int J Antimicrob Agents* **44**:314-319.

- 326 21. **Vumma R, Bang CS, Kruse R, Johansson K, Persson K.** 2016. Antibacterial
327 effects of nitric oxide on uropathogenic *Escherichia coli* during bladder epithelial cell
328 colonization--a comparison with nitrofurantoin. *J Antibiot (Tokyo)* **69**:183-186.
- 329 22. **Forrester MT, Foster MW.** 2012. Protection from nitrosative stress: a central role
330 for microbial flavohemoglobin. *Free Radic Biol Med* **52**:1620-1633.
- 331 23. **McCollister BD, Hoffman M, Husain M, Vazquez-Torres A.** 2011. Nitric oxide
332 protects bacteria from aminoglycosides by blocking the energy-dependent phases of
333 drug uptake. *Antimicrob Agents Chemother* **55**:2189-2196.
- 334 24. **Martinez-Puchol S, Gomes C, Pons MJ, Ruiz-Roldan L, Torrents de la Pena A,**
335 **Ochoa TJ, Ruiz J.** 2015. Development and analysis of furazolidone-resistant
336 *Escherichia coli* mutants. *APMIS* **123**:676-681.
- 337 25. **Darkoh C, Lichtenberger LM, Ajami N, Dial EJ, Jiang ZD, DuPont HL.** 2010.
338 Bile acids improve the antimicrobial effect of rifaximin. *Antimicrob Agents*
339 *Chemother* **54**:3618-3624.
- 340 26. **Anes J, McCusker MP, Fanning S, Martins M.** 2015. The ins and outs of RND
341 efflux pumps in *Escherichia coli*. *Front Microbiol* **6**:587.
- 342 27. **Granik VG, Grigoriev NB.** 2011. Exogenous nitric oxide donors in the series of C-
343 nitro compounds. *Russ Chem Rev* **80**:171-186.
- 344 28. **Baba T, Ara T, Hasegawa M, Takai Y, Okumura Y, Baba M, Datsenko KA,**
345 **Tomita M, Wanner BL, Mori H.** 2006. Construction of *Escherichia coli* K-12 in-
346 frame, single-gene knockout mutants: the Keio collection. *Mol Syst Biol* **2**:2006
347 0008.
- 348 29. **Thomason LC, Costantino N, Court DL.** 2007. *E. coli* genome manipulation by P1
349 transduction. *Curr Protoc Mol Biol* **Chapter 1**:Unit 1 17.

- 350 30. **Datsenko KA, Wanner BL.** 2000. One-step inactivation of chromosomal genes in
351 *Escherichia coli* K-12 using PCR products. Proc Natl Acad Sci U S A **97**:6640-6645.
- 352 31. **Kitagawa M, Ara T, Arifuzzaman M, Ioka-Nakamichi T, Inamoto E, Toyonaga**
353 **H, Mori H.** 2005. Complete set of ORF clones of *Escherichia coli* ASKA library (a
354 complete set of *E. coli* K-12 ORF archive): unique resources for biological research.
355 DNA Res **12**:291-299.
- 356 32. **Green R, Rogers EJ.** 2013. Transformation of chemically competent *E. coli*.
357 Methods Enzymol **529**:329-336.
- 358 33. **Campbell J.** 2010. High-throughput assessment of bacterial growth inhibition by
359 optical density measurements. Curr Protoc Chem Biol **2**:195-208.
- 360 34. **Odds FC.** 2003. Synergy, antagonism, and what the chequerboard puts between them.
361 J Antimicrob Chemother **52**:1-1.
- 362 35. **Doern CD.** 2014. When does 2 plus 2 equal 5? A review of antimicrobial synergy
363 testing. J Clin Microbiol **52**:4124-4128.
- 364 36. **Spagnuolo J, Opalka N, Wen WX, Gagic D, Chabaud E, Bellini P, Bennett MD,**
365 **Norris GE, Darst SA, Russel M, Rakonjac J.** 2010. Identification of the gate
366 regions in the primary structure of the secretin pIV. Mol Microbiol **76**:133-150.
- 367 37. **Cherepanov PP, Wackernagel W.** 1995. Gene disruption in *Escherichia coli*: TcR
368 and KmR cassettes with the option of Flp-catalyzed excision of the antibiotic-
369 resistance determinant. Gene **158**:9-14.

370

371 **Figure legends**

372 **Figure 1: Structural formulae of nitrofurans and Sodium Deoxycholate (E). A)**

373 Furazolidone (FZ); B) Nitrofurantoin (NIT); C) Nitrofurazone (NFZ). D) CM4, Pubchem ID
374 AC1LGLMG (no CAS number). Chemical name: N'-[(5-nitrofur-2-yl)methylidene]furan-
375 2-carbohydrazide or N-[(5-nitrofur-2-yl)methylideneamino]furan-2-carboxamide.

376 **Figure 2: FZ interaction with DOC in growth inhibition of streptomycin- resistant *E.***

377 *coli* K12 (A), ampicillin- and streptomycin-resistant *E. coli* K12 (B), *Salmonella enterica*
378 *sv. Typhimurium* LT2 (C), *Citrobacter gillenii* (D) and *Klebsiella pneumoniae* (E).

379 Graphs (isobolograms) are obtained using a checkerboard analysis at multiple concentration
380 of molecules. Each data point represents the minimum molecule concentrations alone or in
381 combination causing 90 % inhibition to bacterial growth.

382 **Figure 3: Time- kill analysis of the DOC and FZ combination in killing *E. coli* strain**

383 **K1508 (A) and *Salmonella enterica sv. Typhimurium* LT2 (B).** The data is presented as the
384 mean \pm standard error of the mean (SEM) of three independent measurements. The count of
385 the live cells was determined at indicated time points by titration of colony-forming units on
386 agar plates. The lower limit of detection was 60 CFU/mL.

387 **Figure 4: Effect of the $\Delta tolC$ and $\Delta acrA$ mutations on DOC synergy with FZ, NIT, NFZ**

388 **and CM4 in *E. coli*.** Isobolograms characterizing interactions of DOC with FZ (A), NIT (B),
389 NFZ (C) and CM4 (D) in growth inhibition assays of the *E. coli* K12 strain K1508 (WT or
390 wild-type and two isogenic deletion mutants, $\Delta acrA$ and $\Delta tolC$). Each data point corresponds
391 to the FIC (ratios of the 90% growth inhibition concentrations in combination vs. alone) for
392 one of the four nitrofurans (y axis) and DOC (x axis).

393 **Figure 5: Recovery of FZ-DOC synergy in complemented $\Delta tolC$ and $\Delta acrA$ mutants.**

394 Isobolograms of FZ-DOC interactions in growth inhibition of: A. $\Delta tolC$ mutant ($\Delta tolC$) and a
395 derived strain containing a plasmid expressing *tolC* gene ($\Delta tolC + tolC$); B. $\Delta acrA$ mutant
396 ($\Delta acrA$) and a derived strain containing a plasmid expressing *acrA* gene and ($\Delta acrA + acrA$).
397 Each data point corresponds to the FIC (ratios of the 90% growth inhibition concentrations in
398 combination vs. alone) for FZ (y axis) and DOC (x axis).

399 **Figure 6: Effect of the *hmp* gene overexpression on FZ-DOC synergy.** The isobologram
400 of DOC and FZ interaction in *E. coli* having differential expression of NO-detoxifying
401 protein Hmp. WT, strain *E. coli* laboratory strain K1508; WT + *hmp*, K1508 containing a
402 plasmid expressing Hmp under the control of a T5-lac hybrid promoter. Expression of *hmp*
403 gene was induced by IPTG (1 mM). Each data point corresponds to the FIC (ratios of the
404 90% growth inhibition concentrations in combination vs. alone) for FZ (y axis) and DOC (x
405 axis).

406

407 **Tables**

408 **Table 1: Bacterial strains used in this study**

Name	Genotype or description	Source
<i>Escherichia coli</i> <i>O157</i> isolate <i>ERL034336</i>	Human isolate	Dr. Ann Midwinter, School of Veterinary Sciences, Massey University, Palmerston North
<i>Escherichia coli</i>	Isolate from a canine urinary tract infection	New Zealand Veterinary

<i>UPEC P50</i>		Pathology (NZVP)
isolate		diagnostics labs, Palmerston North, New Zealand
<i>Salmonella enterica</i> LT2	Type strain, <i>S. enterica</i> subsp. <i>enterica</i> , serovar Typhimurium	ATCC® 43971™
<i>Citrobacter gillenii</i>	Isolate from a municipal sewage processing (water purification) plant, Palmerston North, New Zealand (classified by complete 16S rRNA sequencing, 99% identity over 1403 nt).	Rakonjac laboratory, Massey University, unpublished.
<i>Klebsiella pneumoniae</i>	Isolate from a municipal sewage processing (water purification) plant, Palmerston North, New Zealand (classified by complete 16S rRNA sequencing; 99% identity over 1403 nt).	Rakonjac laboratory, Massey University, unpublished
<i>Escherichia coli</i> K12 laboratory strains		
K1508	MC4100 [<i>F</i> ⁻ <i>araD</i> ⁻ Δ <i>lac</i> U169 <i>relA</i> ⁻ <i>thiA</i> <i>rpsL</i> (Str ^R)] Δ <i>lamB106</i>	(36)
K2403	K1508 Δ <i>tolC</i>	This study
K2424	K1508 Δ <i>acrA</i>	This study
K2425	K1508 Δ <i>acrA</i> pCA24N:: <i>acrA</i> Δ <i>gfp</i>	This study
K2426	K1508 Δ <i>tolC</i> pCA24N:: <i>tolC</i> Δ <i>gfp</i>	This study
K2524	K1508 pUC118 (Amp ^R)	This study

410

Table 2: List of plasmids used in this study

Name	Genotype or description	Source
pCP20	Amp ^R , Cm ^R , FLP ⁺ , 8 cI857 ⁺ , 8 p _R Rep ^{ts} For removal of an <i>frt</i> -flanked <i>kan</i> marker from <i>E. coli</i> K12 strains by FLP-mediated site-specific recombination	(37)
pUC118	Amp ^R , f1 <i>ori</i> , P _{lacUV5} , <i>lacZα</i>	Creative Biogene, Shirley, NY, USA
pCA24N- <i>tolC</i>	Cm ^R ; <i>lacI^q</i> , pCA24N P _{T5-lac} :: <i>tolC</i> Δ <i>gfp</i>	(31)
pCA24N- <i>acrA</i>	Cm ^R ; <i>lacI^q</i> , pCA24N P _{T5-lac} :: <i>acrA</i> Δ <i>gfp</i>	(31)
pCA24N- <i>hmp</i>	Cm ^R ; <i>lacI^q</i> , pCA24N P _{T5-lac} :: <i>hmp</i> Δ <i>gfp</i>	(31)

411

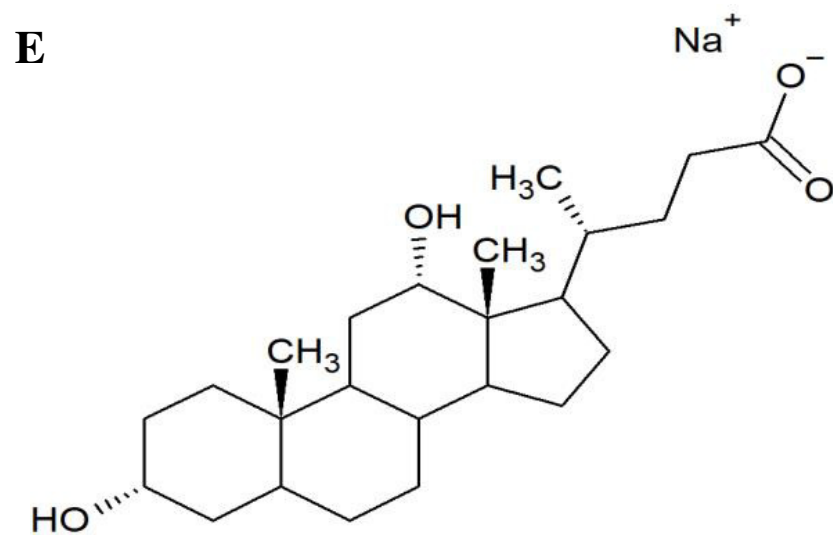
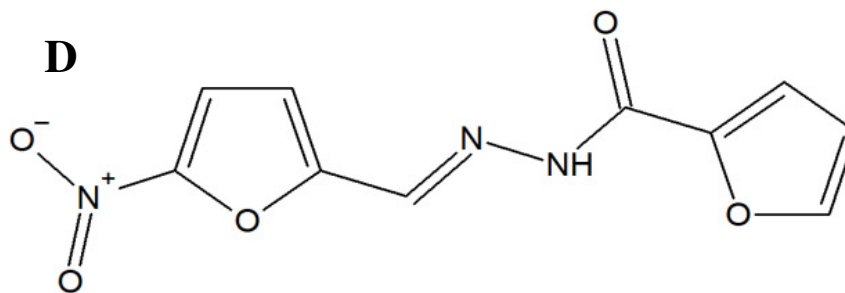
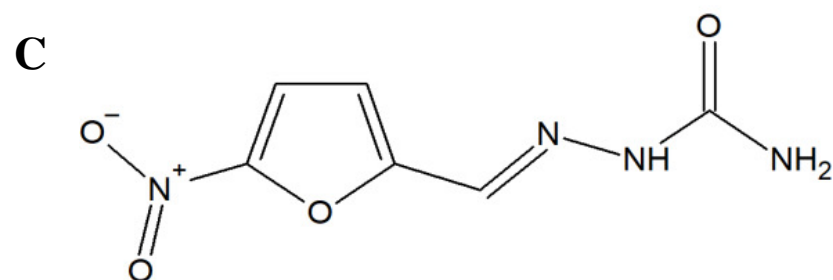
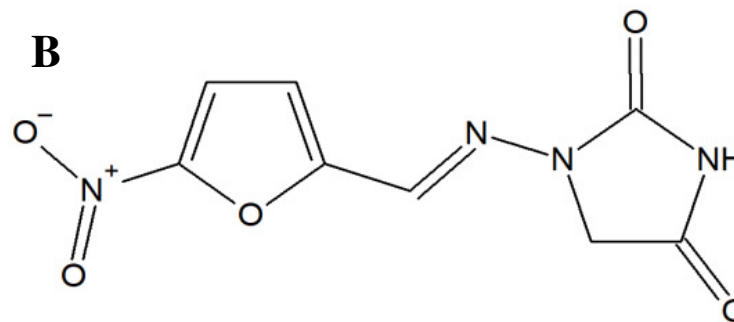
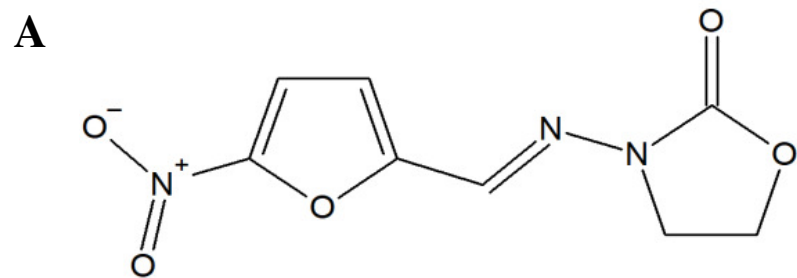


Figure 1

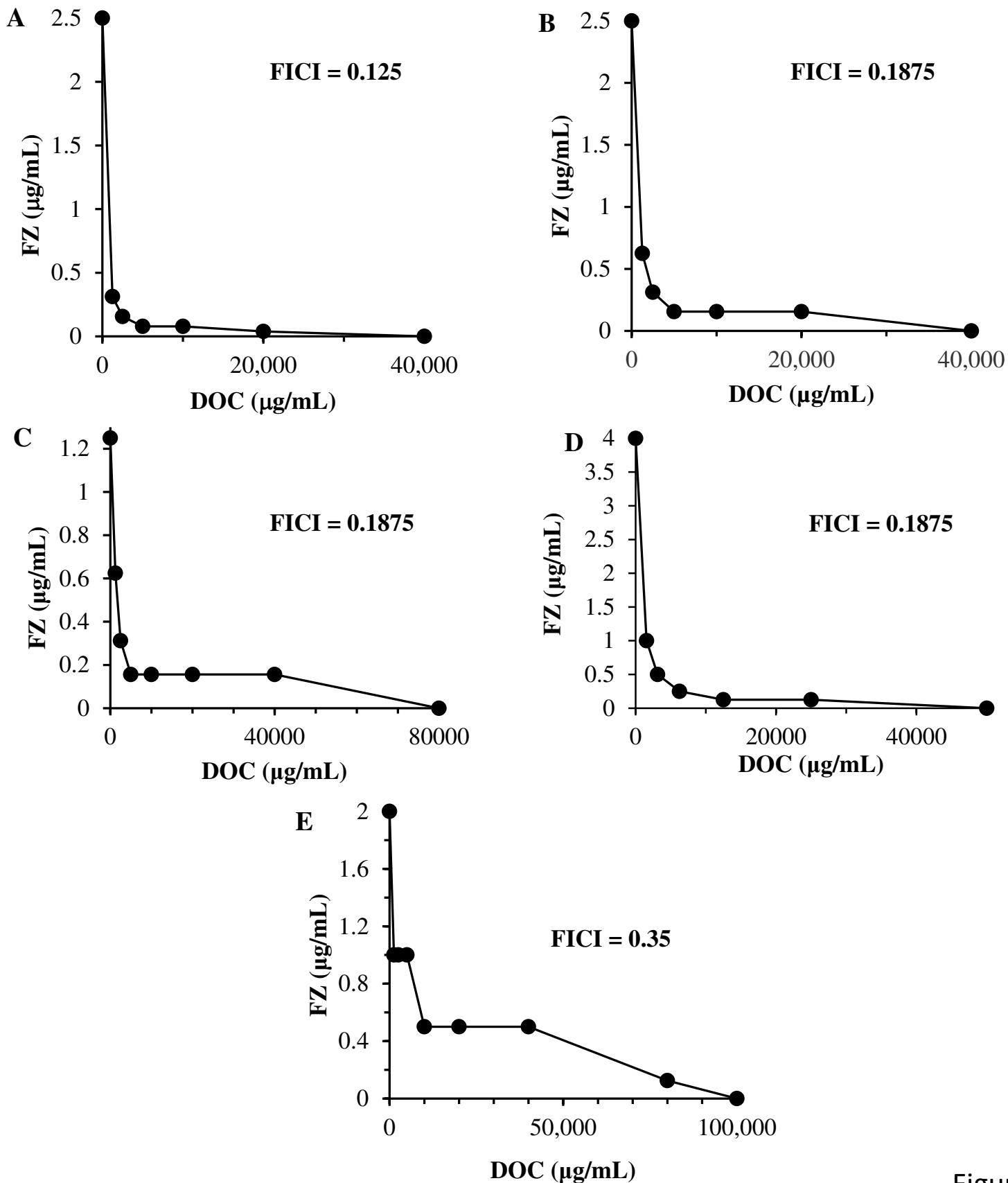


Figure 2

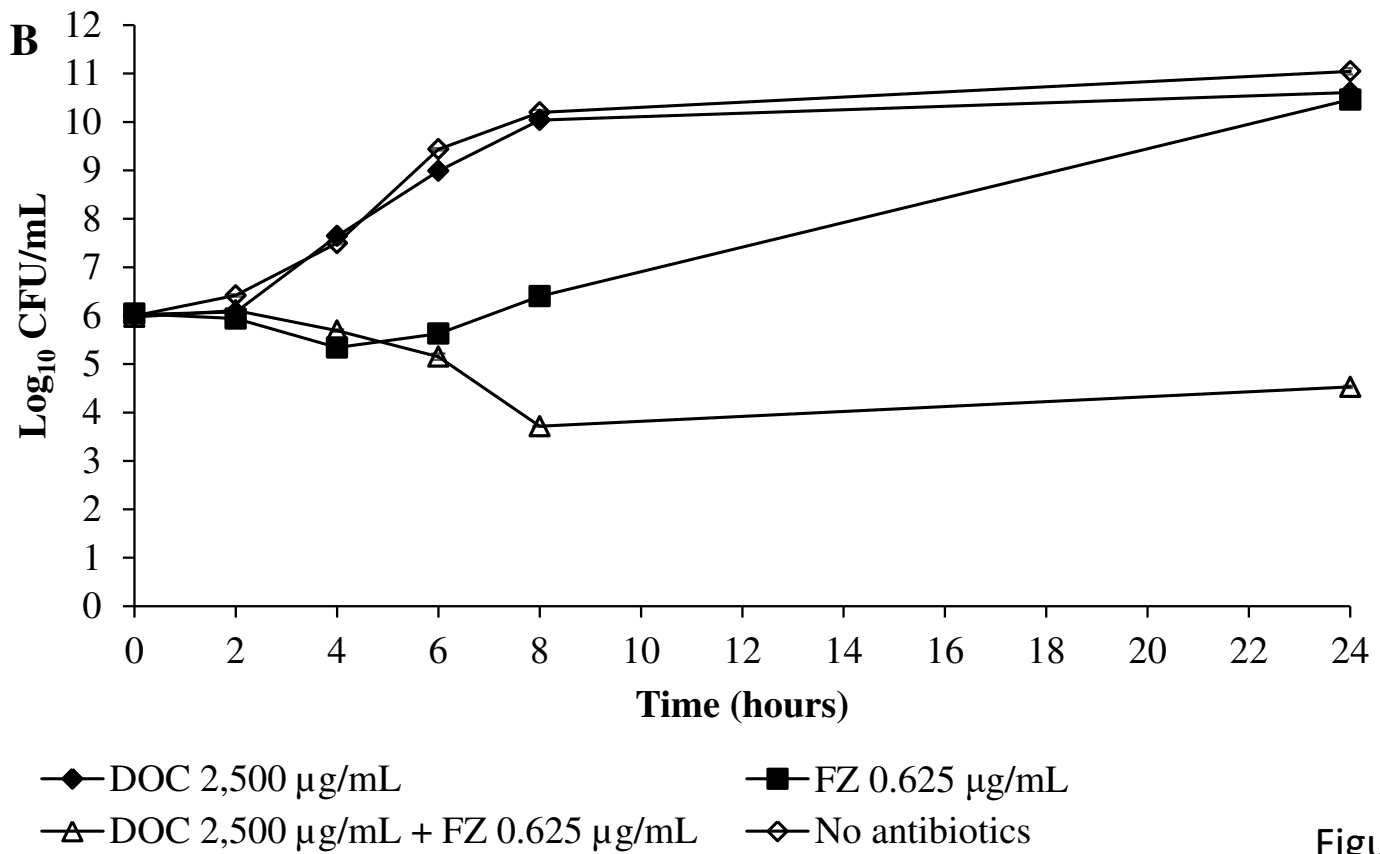
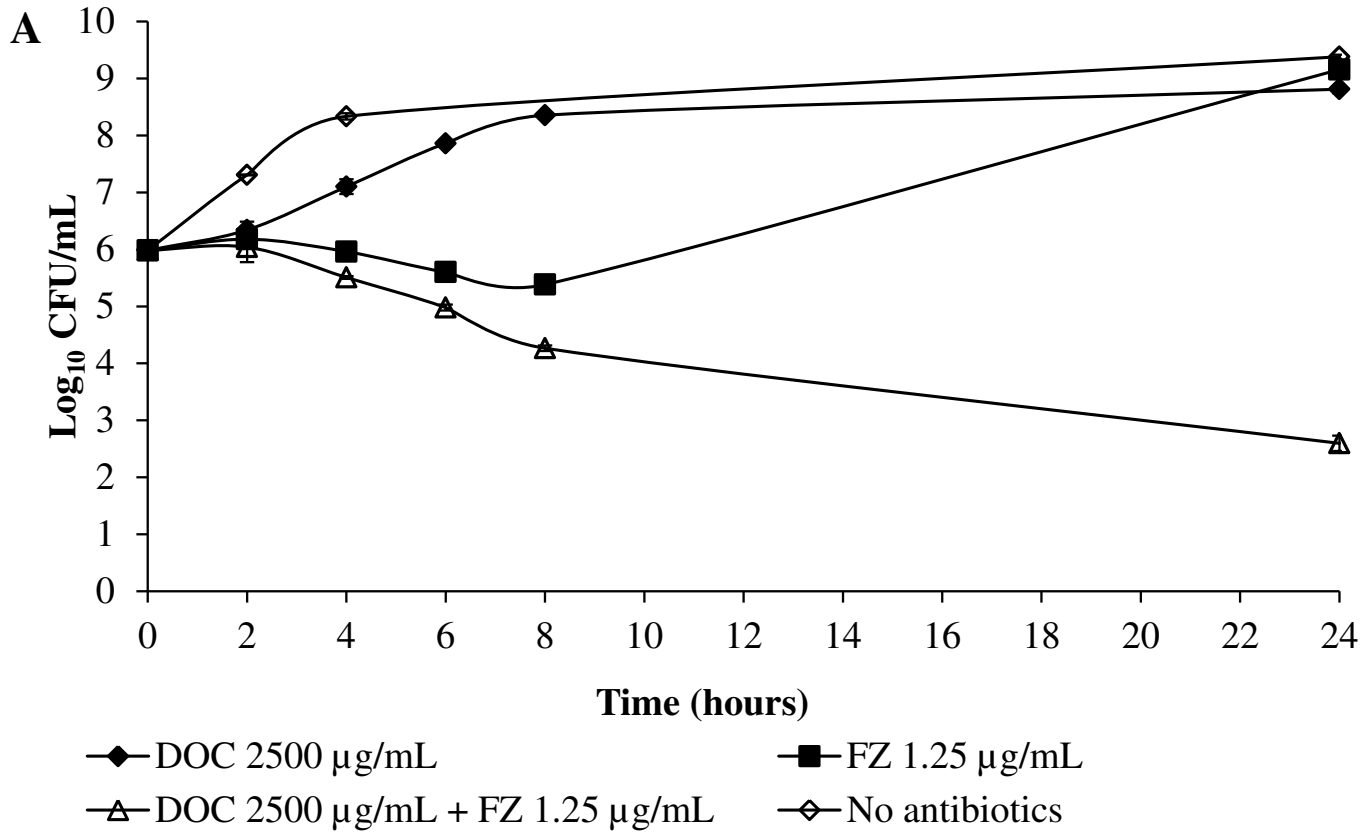


Figure 3

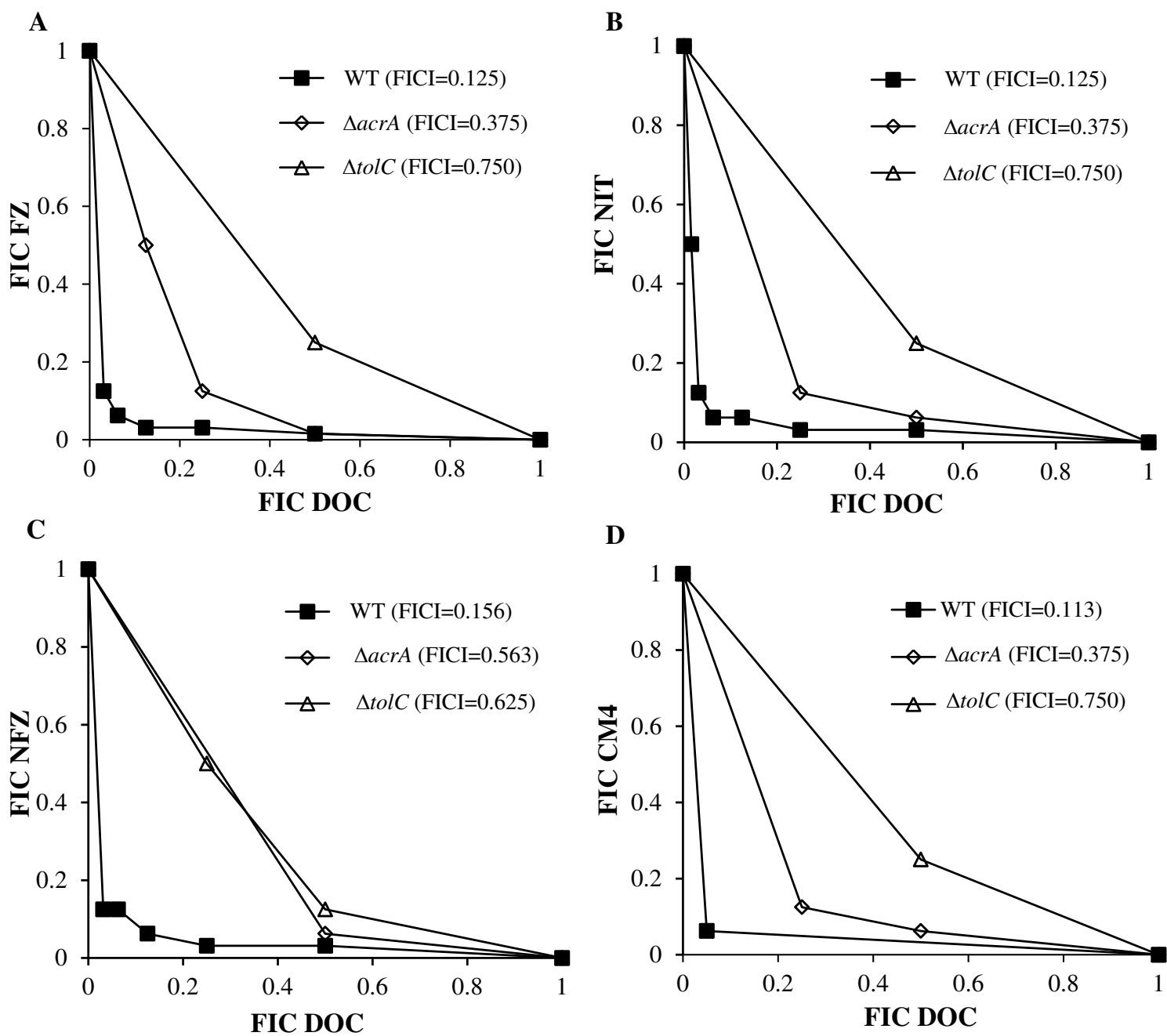


Figure 4

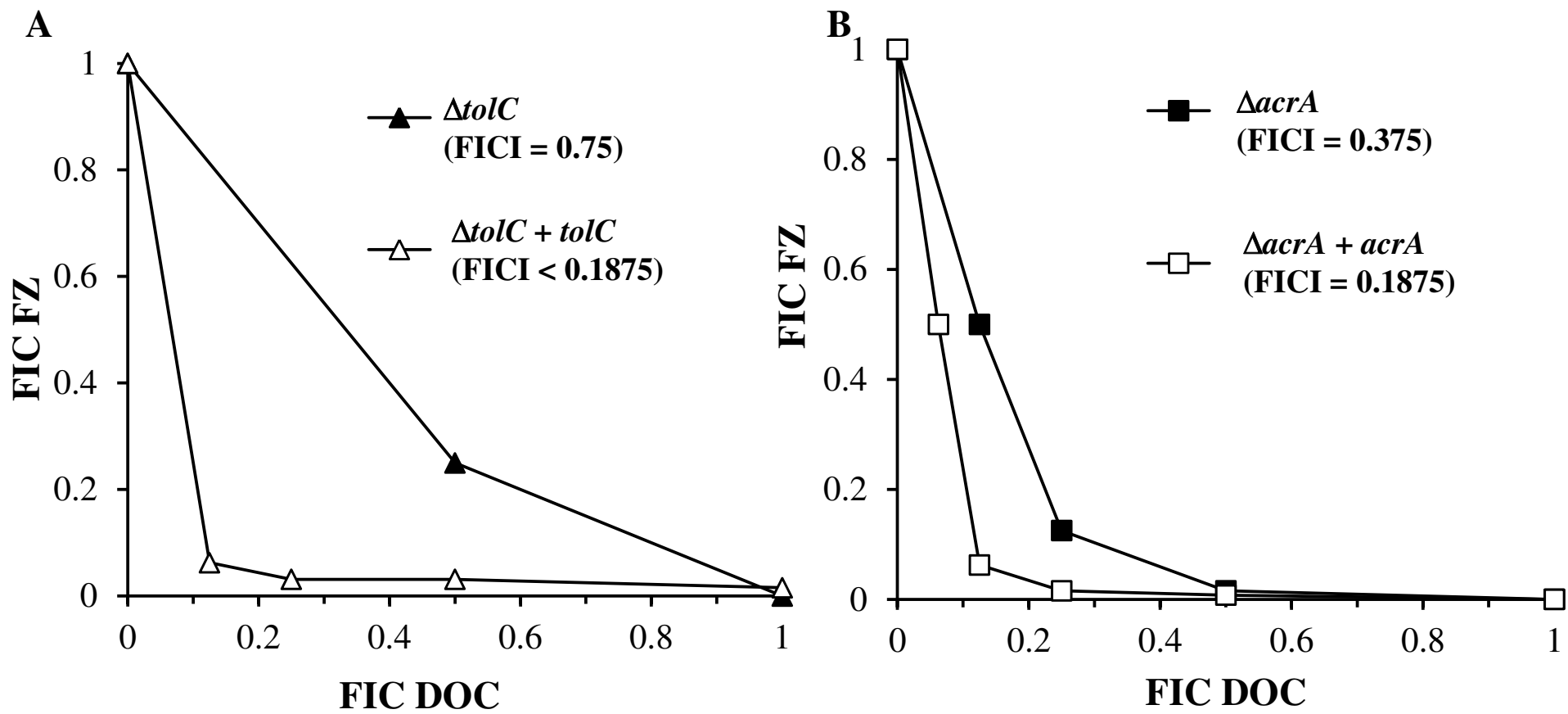


Figure 5

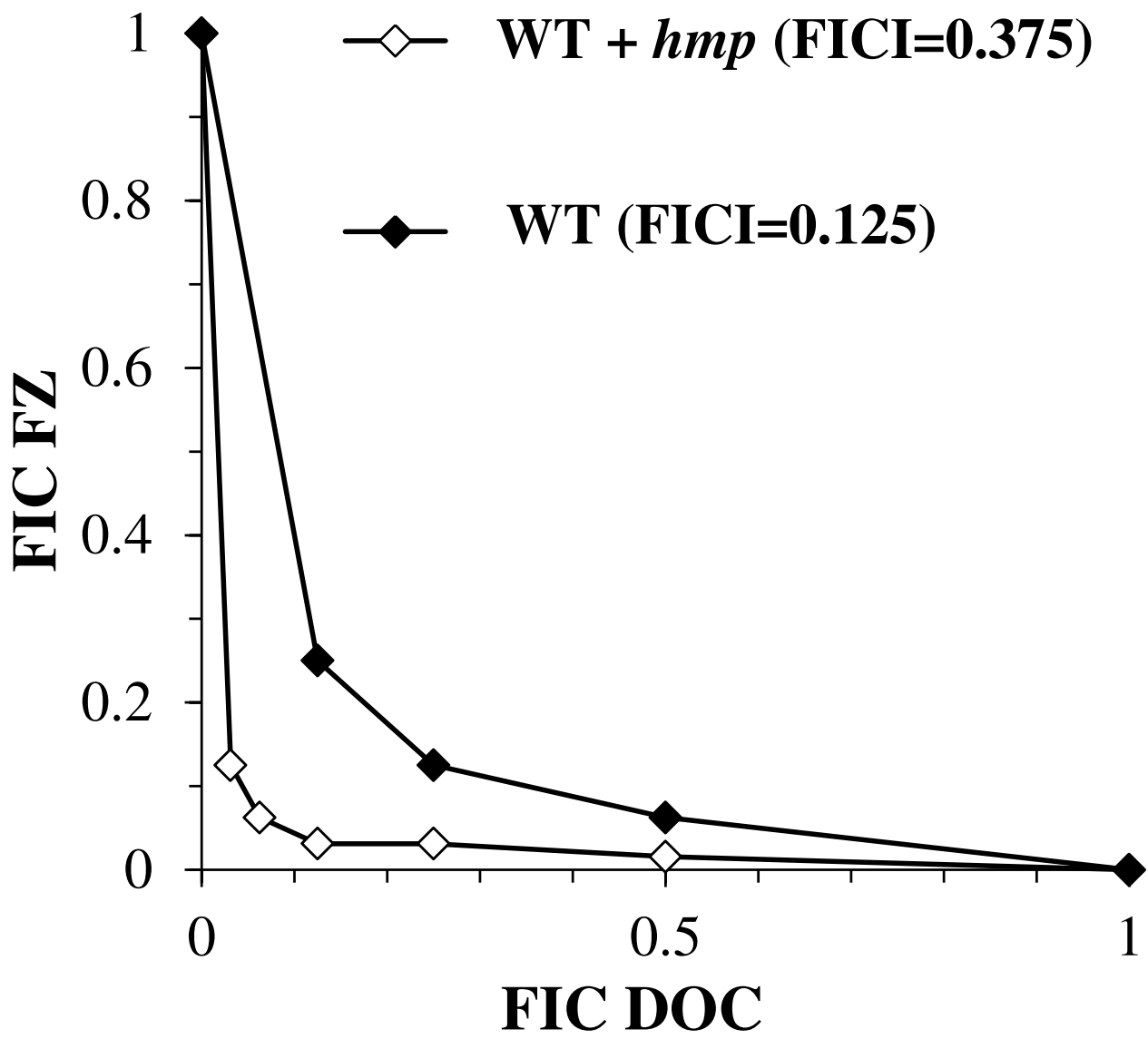


Figure 6